Channels at the Catalytic Site of Glycogen Phosphorylase *b*: Binding and Kinetic Studies with the β-Glycosidase Inhibitor D-Gluconohydroximo-1,5-lactone *N*-Phenylurethane†

D. Barford,‡ J. W. R. Schwabe,‡ N. G. Oikonomakos,§ K. R. Acharya,‡ J. Hajdu,‡ A. C. Papageorgiou,§ J. L. Martin,‡ J. C. A. Knott,‡ A. Vasella,∥ and L. N. Johnson*,‡

Laboratory of Molecular Biophysics, Rex Richards Building, University of Oxford, Oxford OX1 3QU, U.K., The National Hellenic Research Foundation, 48 Vas Constantinou Avenue, Athens 11635, Greece, and Institute of Organic Chemistry, University of Zurich, CH-8057 Zurich, Switzerland

Received April 6, 1988; Revised Manuscript Received May 24, 1988

ABSTRACT: Regions of low packing density in the vicinity of the catalytic site of glycogen phosphorylase *b* are described with the aid of a computer program that generates a contour map in which the contour level is inversely proportional to the packing density in the protein. It is shown that, although there is no direct route from the catalytic site to the surface, there are two possible channels that could allow access for substrates following conformational changes in the enzyme. The first channel, channel 1, leads from the catalytic site to the surface close to the nucleoside inhibitor site and requires movements of residues 280–285 and Arg 569 in order to obtain access. Previous crystallographic experiments have shown that in the presence of substrates or R-state inhibitors these parts of the polypeptide chain undergo large conformational changes. The properties of the second channel (channel 2), which is the more extensive channel, have been investigated with the potent β-glycosidase inhibitor D-gluconohydroximo-1,5-lactone *N*-phenylurethane (PUG). Crystallographic binding studies at 2.4-Å resolution show that the compound binds neatly at the catalytic site of phosphorylase *b*. The glucopyranosylidene ring, in the half-chair conformation, occupies a similar but not identical position (shift about 0.6 Å) to that occupied by other glucosyl compounds bound at the catalytic site. The *N*-phenylurethane extends into channel 2 and makes several favorable contacts to the protein that hold the 280–285 loop in place. Kinetic studies show that PUG is a good inhibitor of phosphorylase (K_i = 0.4 mM) and is directly competitive with the substrate glucose 1-phosphate and noncompetitive with respect to glycogen and AMP. Comparison of the binding interactions between PUG and phosphorylase *b* with those observed for other glucosyl compounds showed no strong interactions that would allow the catalytic site of phosphorylase to distinguish between the chair or half-chair conformation of the glucopyranose ring. Further comparison of PUG binding with that of uridine diphosphate glucose shows that trigonal geometry at the C1 directs the substituent into channel 2, which is available in the T state, while tetrahedral geometry at C1 directs the substituent into channel 1, which becomes available in the R state. It is concluded that the phosphorylase catalytic site provides no dominant steric factors that promote the distortion of the terminal α-D-glucosyl residue from chair to half chair or sofa prior to bond cleavage, a conclusion that is consistent with stereoelectronic theory. It is proposed that the major contribution to the stabilization of the oxocarbonium ion intermediate is mediated through the phosphate of the substrate in a reaction that proceeds by an S_N1 mechanism.

The interior regions of proteins, in general, exhibit similar packing densities to those observed for small molecules in the crystalline state (Lee & Richards, 1971; Richards, 1974). However, within this close-packed framework there are regions of low packing density which result in cavities or crevices that are able to accommodate water molecules or other ligands and that may have no apparent access to the bulk solvent (Richards, 1974; Connolly, 1983; Tilton et al., 1984; Rashin et al., 1986). Such regions of low packing density are of interest, especially for allosteric proteins, in that they allow some fluidity to the protein interior and form possible sites for conformational response. Channels in a protein molecule may be a long-term three-dimensional feature (e.g., membrane ion channels), or they may exist only through the relative flexibility of certain portions of the protein such as the channels that allow access of xenon to the interior site in myoglobin (Tilton et al., 1984). Some information on the possible movements of regions of low packing density have come from studies on the thermal expansion of myoglobin between 80 K and room temperature (Frauenfelder et al., 1987) and protein ligand dynamics simulations (Tilton et al., 1988).

Channels to the catalytic site in glycogen phosphorylase[1] are of interest since increased access to the catalytic site is recognized to form a major part of the allosteric response (Madsen et al., 1978; Withers et al., 1982; Hajdu et al., 1987; Oikonomakos et al., 1988). Glycogen phosphorylase catalyzes the reversible phosphorylation of the α-glycosidic bond at the

† This work was supported by the Medical Research Council and the Science and Engineering Research Council.

* Correspondence should be addressed to this author.
‡ University of Oxford.
§ The National Hellenic Research Foundation.
∥ University of Zurich.

[1] Abbreviations: Glycogen phosphorylase, 1,4-α-D-glucan:orthophosphate α-glucosyltransferase (EC 2.4.1.1); glucose-1-P, α-D-glucopyranose 1-phosphate; heptenitol, 2,6-anhydro-1-deoxy-D-*gluco*-hept-1-enitol; heptulose-2-P, 1-deoxy-D-*gluco*-heptulose 2-phosphate; glucal, 1,5-anhydro-2-deoxy-D-*arabino*-hex-1-enitol; PUG, D-gluconohydroximo-1,5-lactone *N*-phenylurethane; BES, *N*,*N*-bis(2-hydroxyethyl)-2-aminoethanesulfonic acid.

0006-2960/88/0427-6733$01.50/0

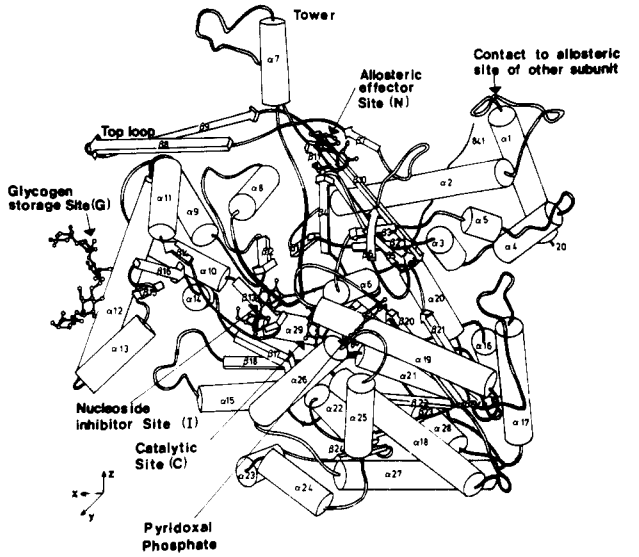

FIGURE 1: Schematic diagram of the phosphorylase *b* monomer viewed down the crystallographic *y* axis. α helices and β strands are shown as cylinders and arrows, respectively. AMP is shown bound at the allosteric site, glucose-1-P and pyridoxal phosphate is at the catalytic site, maltopentaose is at the glycogen storage site, and AMP is at the nucleoside inhibitor site. The loop residues 279–288 between α helices 7 and 8, which partially block access to the catalytic site, are shown shaded.

nonreducing end of glycogen or α-(1–4)-linked oligosaccharides to yield glucose-1-P.

$$(\alpha\text{-1,4-glucoside})_n + P_i \rightleftharpoons (\alpha\text{-1,4-glucoside})_{n-1} + \text{glucose-1-P}$$

The enzyme degrades to within four residues of an α(1–6) branch point in glycogen substrates. In resting muscle the enzyme is in the *b* form and is inactive. It may be converted to the active state either by increased levels of AMP or by reversible phosphorylation to phosphorylase *a* in a mechanism that is under hormonal and neuronal control (Graves & Wang, 1972; Dombradi, 1981; Madsen, 1986; Johnson et al., 1988b).

The crystal structures are available at high resolution of T-state glycogen phosphorylase *b* crystallized in the presence of the weak activator IMP (Sansom et al., 1985; Acharya et al., unpublished results) and T-state phosphorylase *a* crystallized in the presence of the inhibitor glucose (Sprang & Fletterick, 1979). The catalytic site is located in the center of the molecule and incorporates the essential cofactor pyridoxal phosphate (Figure 1). There is no direct access to the site from the bulk solvent. The most likely route has been assumed to lead toward the nucleoside inhibitor site which is located on the surface, but this channel is blocked in the T-state structure mainly by the loop of chain from residue 280 to residue 292 (Figure 1). Crystals of phosphorylase *b* have been shown to be active against oligosaccharide substrates and to exhibit similar K_m values for substrates to those observed under similar conditions in solution (Kasvinsky & Madsen, 1976). Activity in the direction of both oligosaccharide synthesis and breakdown has been observed in time-resolved X-ray crystallographic studies (Hajdu et al., 1987).

An understanding of the phosphorylase mechanism requires knowledge of the stereochemistry of the binding sites for both substrates. Crystallographic studies have clearly shown the location of glucose-1-P and related compounds at the cataltyic site of phosphorylase *b* (Johnson et al., 1980; Jenkins et al., 1981; McLaughlin et al., 1984; Hajdu et al., 1987). However, no binding of the oligosaccharide component at the catalytic site has been observed even with concentrations as high as 1 M. [Instead, oligosaccharides bind strongly to the glycogen storage site on the surface of the enzyme which is some 30 Å from the catalytic site (Figure 1) (Kasvinsky et al., 1978a; Goldsmith et al., 1983; Johnson et al., 1983, 1988a).] Since the enzyme is active in the crystal, it is assumed that the oligosaccharide channel to the catalytic site can open, at least transiently, but not for sufficiently long periods to allow binding to be observed in crystallographic experiments. In studies with the potent product inhibitor, heptulose-2-P, which has certain features of a transition-state analogue (Hajdu et al., 1987), and with the R-state inhibitor uridine diphosphate glucose (Oikonomakos et al., 1988), significant and well-defined conformational changes were observed for the 280–292 loop and other residues at the catalytic site that result in an opening of the channel. In an attempt to further define routes to the catalytic site, the present study reports a computer program that allows channels to be displayed in a form suitable for molecular model building and describes the binding and kinetics of a potent β-glucosidase inhibitor, D-gluconohydroximo-1,5-lactone *N*-phenylurethane.

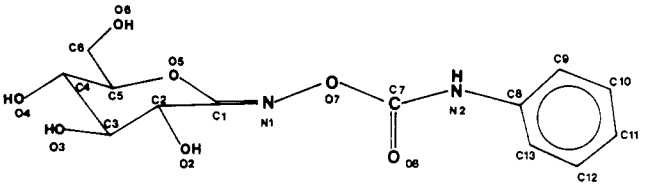

FIGURE 2: D-Gluconohydroximo-1,5-lactone *N*-phenylurethane, showing the numbering scheme.

D-Gluconohydroximo-1,5-lactone *N*-phenylurethane (PUG) (Figure 2) inhibits the β-glucosidase activity of emulsin with a $K_i = 2 \times 10^{-6}$ M (Beer & Vasella, 1986). It was shown from NMR measurements that the lactone moiety of PUG adopts a half-chair conformation similar to that observed for D-gluconolactone in the crystalline state (Hackert & Jacobson, 1971). Its inhibitory properties were ascribed to its ability to resemble the oxocarbonium ion transition-state intermediate on the reaction pathway of β-glycoside hydrolysis. In fact, PUG was a 16-fold better inhibitor of emulsin than D-gluconolactone, and the extra inhibitory properties were assumed to be due to additional interactions made by the *N*-phenylurethane component. The compound provides a larger molecule than has hitherto been available for the exploration of the channels at the catalytic site of phosphorylase *b* and one which is less bulky than an oligosaccharide. It further allows an analysis of the preference of the catalytic site for half-chair or chair geometries. The results are discussed with reference to proposals for the catalytic mechanism.

MATERIALS AND METHODS

Channels Program. The program generates a contour map in which the contour level is inversely proportional to the packing density of the protein in the crystal. A grid with spacing of 1 Å was established and the proximity of atoms to each grid point determined. If the grid point was within a van der Waals radius of any atom, it was assumed to represent a region of high packing density and was assigned a value of zero. All atoms were given a van der Waals radius of 1.5 Å. When a grid point was greater than 1.5 Å from the closest atom, the grid point was assumed to be within a protein cavity and assigned a positive density value. Grid density values were set at arbitrary values of 200 for grid–atom distances greater than 1.5 Å; 400 for 2.5 Å; 600 for 3.5 Å; and 800 for 4.5 Å. The program output consisted of a direct access file of integers, where the grid coordinate was stored as the integer position in the file and the grid density as the integer size. Contouring of the map was performed by the program MAPBRICK (P. R.

Evans, modified by D. I. Stuart). The final contour map was viewed interactively by the program FRODO (Jones, 1978), implemented on an Evans and Sutherland PS300. A 1-Å grid of dimensions 80 × 80 × 72 was used for one monomer of phosphorylase. The cpu time required was 132 min on a Vax 11/750. Symmetry-related atoms within these dimensions were included. The rather coarse 1-Å grid results in a possible underestimate of the cavity to protein distance with a maximum error of 2 Å in any of the x, y, or z directions. The 1-Å grid was found to be sufficiently precise for the present work. Greater precision could be achieved with a smaller grid size requiring greater computing times and storage.

Binding Study with D-*Gluconohydroximo-1,4-lactone N-Phenylurethane.* Rabbit muscle phosphorylase *b* was prepared by the method of Fischer and Krebs (1962). The preparation of D-gluconohydroximo-1,5-lactone *N*-phenylurethane (PUG) has been described by Beer and Vasella (1985). All other chemicals were obtained from Sigma Chemical Co. Crystals were grown from a solution containing 20 mg/mL phosphorylase *b*, 2 mM IMP, 10 mM *N*,*N*-bis(2-hydroxyethyl)-2-aminoethanesulfonic acid (BES), 10 mM magnesium acetate, 3 mM DTT, and 0.02% sodium azide, pH 6.7. The crystals are tetragonal, space group $P4_32_12$, with unit cell dimensions $a = b = 128.5$ Å and $c = 116.3$ Å and contain one phosphorylase subunit (M_r 97 434; 842 amino acids) per asymetric unit with the two subunits of the active dimer related by the 2-fold axis of symmetry at $z = 1/2$ (Johnson et al., 1974). Crystals were transferred from mother liquor to crystallization buffer solution (as above without protein) and soaked in this buffer containing 100 mM PUG for 1.25 h.

Three-dimensional data to 2.4-Å resolution were collected at the Synchrotron Radiation Source, Daresbury, by using an Arndt Wonacott oscillation camera on station 9.6 (Helliwell et al., 1986). The source was operated at 2 GeV, with the wiggler magnet at 5 T and the current varied from 305 to 214 mA. The wavelength from the silicon monochromator was 0.86 Å. Exposure times for a crystal of dimensions 0.3 × 0.26 × 2.2 mm^3 were 50 s/deg. Each photograph was recorded for an oscillation range of 1.5°, and the total rotation was 46.5° for a crystal mounted about $c(c^*)$. The crystal was translated twice during data collection to relieve radiation damage. Films were scanned on a Joyce-Loebl Scandig 3 microdensitometer and the intensities integrated with profile fitting by using a modified version (D. I. Stuart, unpublished work) of the MOSCO data-processing programs (Nyborg & Wonacott, 1977) implemented on a PDP11/70 or Vax 11/750 computer. Data were corrected for oblique incidence, Lorentz polarization factors, and intrafilmpack scaling. Data from each oscillation range were scaled and symmetry-related reflections merged. The final data set consisted of 133 506 measurements, which were reduced to a unique data set of 32 407 reflections with a merging residual on intensities of 0.082. [The merging residual is defined as $\sum_i\sum_h|\bar{I}(\bar{h}) - I_i(h)|/\sum_i\sum_h I_i(h)$, where $I_i(h)$ is the ith measurement of the intensity of reflection h and $\bar{I}(\bar{h})$ is the mean of these measurements.] The data were scaled to the native data set. The mean fractional isomorphous change was 0.173. The difference Fourier synthesis was based on coefficients $m(F_L - F_P)$ and calculated phases, where F_L and F_P are the structure factor amplitudes of the ligand-bound and native protein, respectively, and m is the figure of merit associated with the calculated phases from the refined native structure. The current crystallographic R factor for the refined model of glycogen phosphorylase *b* is 0.187 for 61 344 reflections ($I > 3\sigma$) to 1.9-Å resolution (K. R. Acharya et al., unpublished results). The number of atoms in the refinement is 7398 including 692 water molecules, and the root mean square deviation from ideal bond length is 0.028 Å. Electron density maps were examined on an Evans and Sutherland PS 300 color graphics device on line to a Vax 11/750 computer with the program FRODO (Jones, 1978, 1985; modified by J. W. Pflugrath, M. Saper, R. Hubbard, and P. R. Evans).

The crystal structure of PUG is not known. A model was constructed by using the energy minimization program COSMIC (written by J. G. Vinter of Smith, Kline and French). The gluconohydroximolactone was modeled with the half-chair conformation previously determined for heptenitol (Hajdu et al., 1987), which is almost identical with that observed for the single-crystal structure of D-gluconolactone (Hackert & Jacobson, 1971) and is consistent with NMR observations (Beer & Vasella, 1986). The oxime link was constructed with C1–N1 and N1–O7 bond lengths 1.33 and 1.35 Å, respectively, and bond angles at N1 and O7 were 110° and 116°, respectively. The urethane and the benzene ring were added with standard stereochemistry. After energy minimization the model was fitted to the electron density by adjustment of bond torsion angles.

Kinetics. Glycogen phosphorylase *b* (5 μg/mL) was assayed in the direction of glycogen synthesis with 1% glycogen, 1 mM AMP, 47 mM triethanolamine hydrochloride, 100 mM KCl, 1 mM dithiothreitol, and 1 mM EDTA, pH 6.8, at 30 °C and a range of concentrations of glucose-1-P and PUG. Enzyme and glycogen were preincubated at 30 °C before initiating the reaction with glucose-1-P. Inorganic phosphate released in the reaction was measured by the method of Fiske and Subbarow (1925), and initial velocities were calculated by the method of Engers et al. (1970). Control activity without inhibitor was 58 μmol/(min·mg) at 20 mM glucose-1-P. A kinetic analysis was also carried out in the presence of 0.5 mM caffeine, a T-state inhibitor of phosphorylase.

A preliminary analysis of the inhibitory properties of glucose, maltose, and maltotriose was carried out by using a slightly different assay procedure. In this case, phosphorylase (10.64 μg/mL) was assayed in the direction of glycogen synthesis with 0.2% glycogen, 1 mM AMP, 20 mM β-glycerophosphate, 2 mM dithiothreitol, and 0.2 mM EDTA, pH 6.8 at 30 °C. The enzyme and glycogen in the presence of the oligosaccharide inhibitor were incubated at 30 °C before initiating the reaction with glucose-1-P. The final concentrations of glucose-1-P and oligosaccharide in the reaction mixture were 20 and 100 mM, respectively. Inorganic phosphate released in the reaction was measured by the method of Hu and Gold (1975), and initial velocities were calculated by the method of Engers et al. (1970).

RESULTS

Channel Program. By contouring regions of low packing density, the program enables channels and cavities to be highlighted. Model building to cavities is facilitated since the molecule can be fitted to the contours in a similar way as to electron density maps. Different contour levels reveal different aspects of atomic packing. The lowest level, 200 (1.5-Å cavities), reveals all regions of low density, including packing defects. Such regions are too small to accommodate atoms in van der Waals contact with the protein. Regions contoured at 400 (2.5 Å) represent cavities large enough to accommodate atoms. Thus at the catalytic site, for example, all the peripheral atoms of the glucopyranose ring approach a protein atom within 2.5–3.5 Å and lie close to the edge of the 400 cavity. Contouring at 600 and 800 (3.5- and 4.5-Å cavities) delineates deep cavities and the protein surface. In phosphorylase the only significant cavity contoured at 600 was the

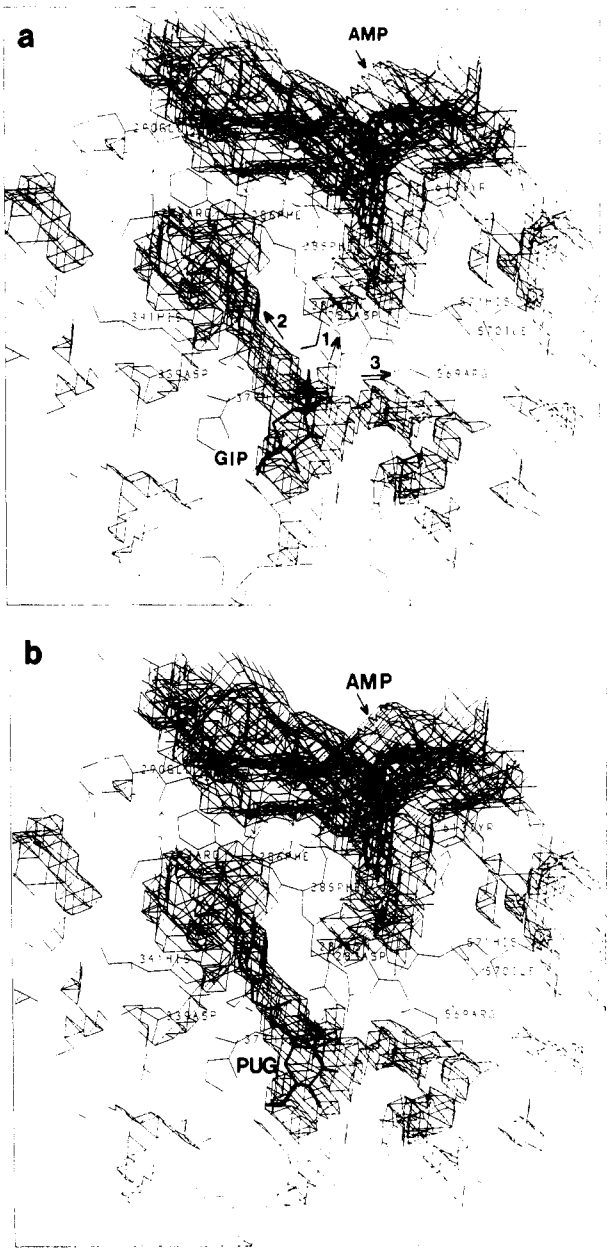

FIGURE 3: Contours at the "2.5-Å" level (see text) produced by the channels program in the vicinity of the catalytic site. (a) Glucose-1-P and AMP are shown at the catalytic and nucleoside inhibitor sites, respectively. (b) PUG and AMP are shown at the catalytic and nucleoside inhibitor sites, respectively. The numbers indicate possible channels.

glucose-1-P binding site close to the center of the molecule. No cavities were contoured at 800.

When the phosphorylase molecule is displayed with the channel program at the "2.5-Å" contour, numerous surface indentations, water-filled enclosed pockets, and water-filled channels were apparent. A detailed description will be given in another manuscript. Here we concentrate on the channels leading to the catalytic site. These are shown in Figure 3a. The extensive contours in the top right of the figure represent the solvent. The position of AMP at the nucleoside inhibitor site is shown bound at a site on the surface located between the aromatic rings of Phe 285 and Tyr 613. The catalytic site itself is marked by the position of glucose-1-P. Its distance from the surface is about 12 Å. The phosphate of the pyridoxal phosphate is adjacent to this major cavity and is partly surrounded by water molecules. It is apparent that there is no direct access from the catalytic site to the solvent. There

Table I: Torsion Angles Observed for the Fit of D-Gluconohydroximo-1,5-lactone *N*-Phenylurethane to the Difference Electron Density[a]

	torsion angle (deg)
O5–C1–N1–O7	−10
C1–N1–O7–C7	−143
N1–O7–C7–N2	−144
O7–C7–N2–C8	−180
C7–N2–C8–C9	51

[a] The numbering system is given in Figure 1.

are three possible routes (marked in the figure), but each of these channels would require conformational changes in the protein in order to reach the surface. Channel 1 leads from the phosphate of glucose-1-P through the side chains of Asp 283, Asn 284, and Arg 569 to reach the solvent interface in the vicinity of the nucleoside site. This channel is blocked by the side chains of Asp 283, Asn 284, and Arg 569. Channel 2 appears the predominant channel in the contour map. It extends between Asp 283, Phe 285, and Phe 286 on one side and Asp 339, His 341, and Arg 292 on the other side, but access to the surface is blocked by the loop of chain 287–292. Its total volume is about 400 Å^3. In the native structure channel 2 is partially filled with five firmly bound water molecules. Channel 2 is wholly within domain 1, but channel 1 is between domains 1 and 2. The two channels are separated by the loop 280–285. Both have a length to the surface that could accommodate 4–5 glucosyl residues. Channel 3 passes between Arg 569 and the pyridoxal phosphate and then between loop 123–133 from domain 1 and loops 567–569, 698–610, and 648–650 of domain 2. This channel is narrow and discontinuous in two places and has a total length equivalent to 7–8 glucosyl units. These properties suggest that the third channel is unlikely to represent the oligosaccharide substrate binding channel but may serve as a region of low packing density that allows some conformational response of the protein.

PUG Binding. The difference electron density map for PUG showed a single major peak at the catalytic site and some small features indicating limited conformational changes (Figure 4). The glucopyranosylidene ring occupies a similar but not identical position to that observed for other glucosyl compounds. The *N*-phenylurethane occupies channel 2 (Figure 3b).

The fit of the model to the electron density is shown in Figure 4. The ligand adopts an extended conformation, and torsion angles are given in Table I. The half-chair conformation of the D-gluconohydroximolactone fits the density well. There is a small deviation from planarity about the C1–N1 bond (torsion angles O5–C1–N1–O7 and C2–C1–N1–O7 are −10° and −178°, respectively). The plane of the phenyl ring is approximately normal (94°) to the plane of the gluconohydroximolactone ring and inclined 52° to the plane of the urethane group. The conformation appears to be stabilized by intermolecular contacts to the protein, and there are no intramolecular hydrogen bonds.

The difference Fourier map indicates some small, local conformational changes. His 377 shifts away from the C6–O6 group of the glucopyranosylidene ring, a shift that is observed with all glucose-like molecules bound at the catalytic site in phosphorylase *b*. The movement of His 377 results in small shifts in Asn 338, which is hydrogen bonded to His 377 and to Tyr 374 and Thr 375, which are in van der Waals contact with His 377. The only other shift observed is for Asn 284, which moves slightly to avoid too close a contact with the ligand.

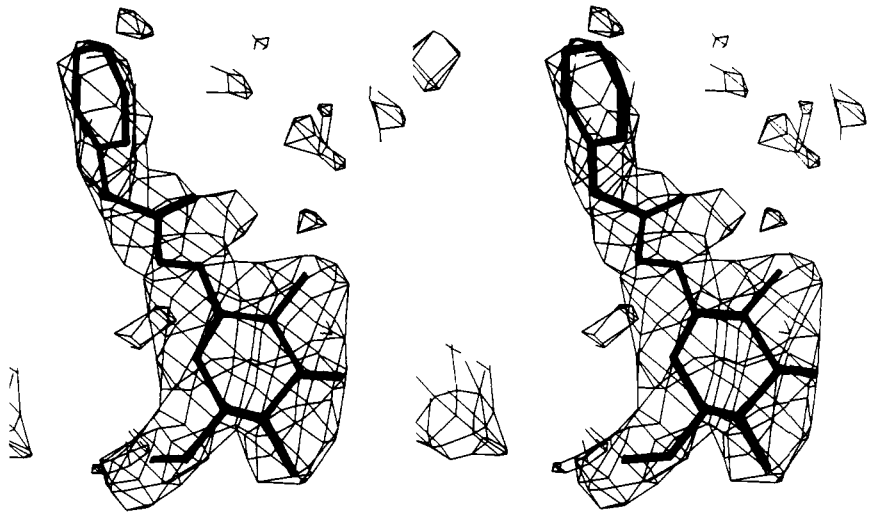

FIGURE 4: Stereo diagram showing the fit of PUG to the difference electron density at the catalytic site. Positive contours (300 arbitrary units) only are shown.

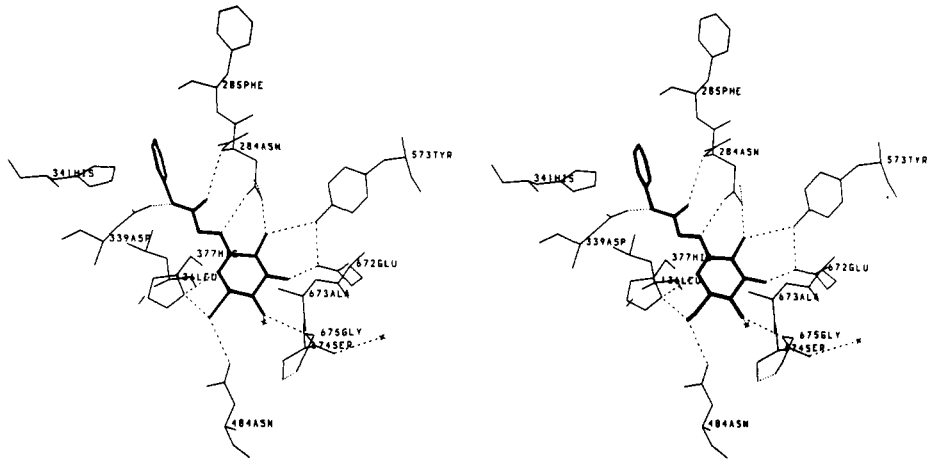

FIGURE 5: Stereo diagram of the contacts between phosphorylase *b* and PUG. Gly 135 has been omitted for clarity.

The contacts between the protein and the ligand are shown in Figure 5 and Table II. In total there are some 94 van der Waals interactions ≤4 Å and 11 hydrogen bonds between the ligand and the protein. All the peripheral hydroxyl groups of the glucopyranosylidene ring are involved in hydrogen bonds, and these interactions are typical (with some small variations) of the contacts made by other glucose and glucosyl derivatives at this site. The remainder of the ligand fits neatly into the pocket of channel 2 and makes some remarkably specific contacts. The N1 atom is within hydrogen-bonding distance (2.8 Å) of OD1 Asn 284, but a hydrogen bond could only be made if the N1 atom was protonated. (The ND2 atom of Asn 284 is involved in a hydrogen bond with the OD2 atom of Asp 283.) The O8 and N2 atoms of the urethane link are involved in hydrogen bonds with Asn 284 (main-chain nitrogen) and Asp 339 (OD1), respectively. The phenyl ring makes good van der Waals contacts to loop 282–285 on one side and Leu 136 and His 341 on the other side. The planes of the histidine and phenyl rings are almost perpendicular, and it seems likely that this contact is stabilized by the interaction of the histidine protons with the π electrons of the phenyl ring. There is one short contact between N2 and the CD1 atom of Leu 136 (2.1 Å). This short contact could be alleviated by a small movement of the side chain although there is no indication for such a shift in the difference map.

To date, the binding of nine glucosyl analogues has been studied at the catalytic site of phosphorylase *b* [glucose-1-P

Table II: Hydrogen Bonds and van der Waals Contacts between PUG and Phosphorylase *b*

		H Bonds			
O2	ND2	Asn 284	O6	ND1	His 377
	OH	Tyr 573		OD1	Asn 484
O3	OE1	Glu 672	N1	OD1	Asn 284
O4	N	Gly 675	O8	N	Asn 284
	OH_2	Wat 897	N2	OD1	Asp 339
O5	ND1	His 377			

van der Waals Contacts (<4 Å)	
C1	Asn 284, His 377
C2	Asn 284, His 377, Glu 672
O2	Asn 284, His 377, Tyr 573, Glu 672
C3	Glu 672
O3	Tyr 573, Glu 672, Ser 674, Gly 675
C4	Gly 675, OH_2 897
O4	Asn 484, Ser 674, Gly 675, OH_2 897
C5	Gly 135, Leu 135, His 377, OH_2 897
O5	Leu 136, His 377
C6	Gly 135, His 377, Asn 484, OH_2 897
O6	His 377, Asn 484
N1	Asn 284, His 377, Thr 378
O7	Leu 136, Asn 284, His 377
C7	Leu 136, Asn 284
O8	Leu 136, Asn 284
N2	Leu 136, Asp 339, His 341
C8	Leu 136, Asp 339, His 341
C9	Leu 136, Asn 282, Asn 284, His 341
C10	Asn 282, Asp 283, Asn 284, His 341
C11	Asn 282, Phe 285, His 341
C12	Phe 285
C13	Leu 136, Asp 339, His 341

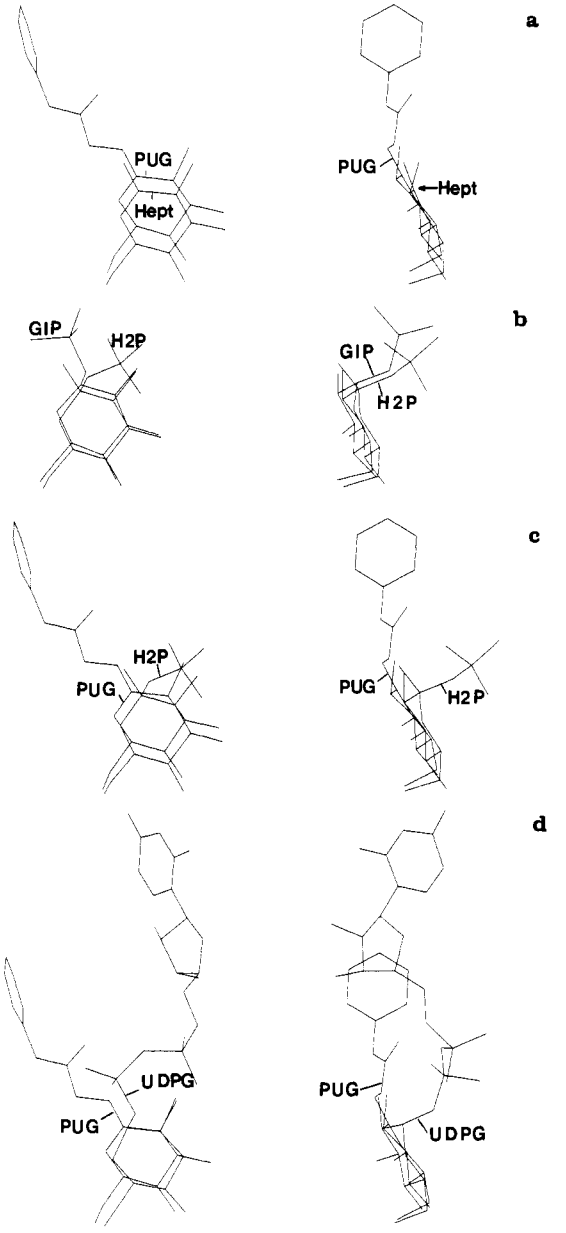

FIGURE 6: Orthogonal views of the positions of various glucosyl compounds bound at the catalytic site. (a) Half-chair compounds: heptenitol and PUG. (b) Chair compounds: heptulose-2-P and glucose-1-P. (c) Heptulose-2-P and PUG. (d) Uridine diphosphate glucose and PUG.

(Johnson et al., 1980), glucose 1,2-cyclic phosphate (Jenkins et al., 1981), heptenitol (McLaughlin et al., 1984), heptulose 2-phosphate (Hajdu et al., 1987), glucose (Oikonomakos et al., 1987), uridine diphosphate glucose (Oikonomakos et al., 1988), deoxynorjirimicin (Johnson et al., unpublished results), glucal (J. L. Martin, unpublished results), and PUG (present work)]. The positions of heptenitol and glucal, the two smaller compounds with trigonal geometry at C1 and half-chair geometry, superimpose closely. PUG differs in its ring position from these compounds (Figure 6a). The shift is about 0.6 Å toward the surface. Glucose, glucose-1-P, and heptulose-2-P, three compounds with chair conformation of the glucopyranose ring, show some differences in their respective positions (Figure 6b). However, heptenitol and heptulose-2-P show greater similarity than PUG and heptulose-2-P (Figure 6c). The two larger compounds, uridine diphosphate glucose and PUG, show similar positions for their glucosyl components (Figure 6d). Thus glucosyl residues with half-chair or chair geometry bind

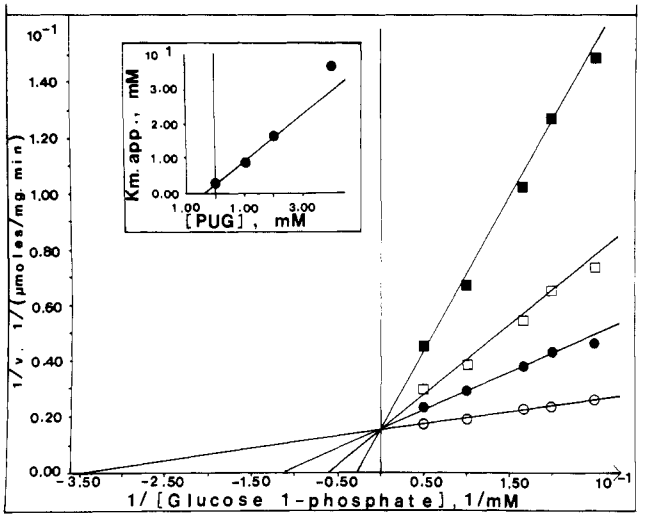

FIGURE 7: Lineweaver–Burk plot of PUG inhibition of phosphorylase *b* at constant AMP (1 mM) and glycogen (1%) concentrations. PUG concentrations are as follows: (○) none; (●) 1 mM; (□) 2 mM; (■) 4 mM. Inset: Replot of the apparent K_m values against inhibitor concentration.

Table III: Synergistic Inhibition of Phosphorylase *b* Activity by PUG and Caffeine

PUG (mM)	inhibition (%) without caffeine	inhibition (%) with caffeine (0.5 mM)	PUG (mM)	inhibition (%) without caffeine	inhibition (%) with caffeine (0.5 mM)
0	0	19.7	2.0	34.2	65.3
0.5	10.6	36.1	3.0	45.9	75.4
1.0	20.2	50.4			

in approximately the same positions at the catalytic site, but those compounds with bulky substituents at C1 (PUG and uridine diphosphate glucose) exhibit greater displacement. A half-chair geometry for the glucosyl residue makes little difference to the contacts to the enzyme compared with a chair geometry, but it does influence the direction in which the substituent is forced to lie as can be seen by comparing the positions for uridine diphosphate glucose and PUG in Figure 6d.

Kinetics. Kinetic studies of the inhibition of rabbit muscle phosphorylase by PUG showed that it is a good inhibitor of the enzyme, directly competitive with glucose-1-P. The Lineweaver–Burk plot for phosphorylase *b* in the presence of different concentrations of PUG is shown in Figure 7. A K_i value of 0.4 mM for the enzyme–glycogen–AMP–PUG complex was obtained from a replot of the apparent K_m for glucose-1-P in the presence of each concentration of inhibitor (Figure 7, inset). The effect on the inhibitor binding of the nucleotide activator (AMP) and the other substrate, glycogen, was also studied (data not shown). Results obtained from these experiments showed noncompetitive inhibition of PUG with respect to both AMP and glycogen, and when the data were analyzed by assuming that the reaction proceeded through a random bi-bi kinetic mechanism, an inhibition constant of 0.5 mM was calculated for the enzyme–AMP–PUG complex.

Glucose and caffeine stabilize the T state of phosphorylase and synergistically inhibit the enzyme (Kasvinsky et al., 1978b). The kinetic data on the inhibition by PUG in the presence of caffeine are shown in Table III. The combined PUG and caffeine inhibitions are more than the sum of the inhibitions produced by either compound separately. Dixon plots of reciprocal velocity versus PUG concentration at different fixed caffeine concentrations provided intersecting lines

Table IV: Inhibition of Phosphorylase *b* Activity by Oligosaccharides

inhibitor	concn (mM)	act. [μmol/(mg·min)]	% inhibition
		64	
glucose	100	17	73
maltose	100	58	9
maltotriose	100	39	39

with an interaction constant $\alpha = 1$, indicating that the binding of one inhibitor does not affect the binding of the other (Segal, 1975).

Kinetic studies on the inhibition of phosphorylase by oligosaccharides showed that, in comparison to glucose, maltose and maltotriose are poor inhibitors (Table IV). At 100 mM concentration, maltose produced only 9% inhibition compared with 73% inhibition produced by glucose under the same conditions. Maltotriose showed improved inhibitory properties compared to maltose but still only gave 39% inhibition.

Discussion

The studies with the channels program have highlighted the remarkably large solvent-filled enclosed channels adjacent to the catalytic site of phosphorylase *b*. They show that there are two possible routes to the surface, both of which require conformational changes in the loop residues 280–292. The potent β-glycosidase inhibitor, PUG, was found to bind to one of these channels. The ligand makes a number of successful contacts to the protein both with its glucosyl moiety, for which phosphorylase has a definite recognition site, and with the *N*-phenylurethane moiety, which makes 2 good hydrogen bonds and some 51 van der Waals interactions, including a favorable interaction with a histidine residue. The contacts to the *N*-phenylurethane are remarkable because the protein has no biological reason to recognize this component. The results provide a further demonstration of the existence of sites in protein molecules that can adventitiously bind nonbiological ligands. This feature and the ability to identify such sites are important for the design of specific drugs with desired properties (Hol, 1986). The channels program described in this paper shows that a larger ligand than PUG could be accommodated in the pocket (Figure 3b) and illustrates the usefulness of the program in identifying such sites and in providing guiding contours for molecular model building.

The low affinity for oligosaccharide substrates exhibited by T-state phosphorylase in the tetragonal crystals is undoubtedly associated with the lack of access to the catalytic site from the solvent. Both of the potential surface channels 1 and 2 are blocked by the loop of chain 278–292. In the native enzyme this loop is well located even though it is partly sandwiched by the channels. The isotropic temperature factors determined in the course of the crystallographic least-squares refinement for the main-chain atoms and most of the side-chain atoms are close to the root mean square temperature factor for the whole protein, and the electron density is well-defined. This is not surprising because most of the loop makes specific contacts with the protein (Figure 1). At its amino terminal the loop is held by the tower helix (α 7; residues 261–274). This helix forms a major part of the subunit–subunit interactions in the protein through its contacts to the symmetry-related antiparallel α 7 helix of the other subunit. Residues 276–279 are involved in a short stretch of β sheet with residues 161–163. The main-chain N of Tyr 280 is linked via a water molecule to the side chain of Glu 295 and Arg 292 and the Tyr 280 peptide oxygen to the side chain of Asn 133. The peptide oxygen of Pro 281 is hydrogen bonded to the side chain of Arg 569. Residues 282–285 show no main-chain hydrogen bonds, but the side chains of Asn 282, Asp 283, and Asn 284 are each involved in hydrogen bonds. The main-chain N of Phe 286 is hydrogen bonded to the carbonyl oxygen of Glu 382, and the following residues 287–289 are involved in a reverse γ turn. The chain then enters α helix 8 (residues 289–314), the helix that contributes to the allosteric effector site through the two arginine residues, Arg 309 and Arg 310. Thus movement of the loop must result in disruption of contacts to other parts of the protein. Large conformational changes in this region were first observed in crystals of phosphorylase *a* on incubation with substrate mixtures in a study at 6-Å resolution (Madsen et al., 1978). In phosphorylase *b* dramatic shifts in this region have been observed in two crystallographic binding studies. On formation of the potent inhibitor product, heptulose 2-phosphate, the side-chain Arg 569 was observed to move into the catalytic site to make contact with the product phosphate, and simultaneously residues 281–285 were displaced by a pivotal movement around Pro 281 (Hajdu et al., 1987) and other residues were also shifted. In the 2.5-Å studies with the R-state inhibitor uridine diphosphate glucose, the whole of the loop from residue 279 to residue 288 is displaced and apparently becomes mobile (Oikonomakos et al., 1988). These observations provide strong evidence for the proposals [reviewed by Johnson et al. (1988b)] that a major feature of the T to R transition in phosphorylase involves the displacement of the loop and, through movement of Phe 285, subsequent destruction of the nucleoside inhibitor site. The present observations that PUG binds at the catalytic site without displacement of the loop and indeed makes interactions that favor the interior position of the loop therefore indicate that PUG should be a T-state inhibitor.

The kinetic experiments show that PUG is a good inhibitor of phosphorylase with an inhibition constant of 0.4 mM for the enzyme–AMP–glycogen complex. Under similar conditions the inhibition constant for glucose is 2.0 mM (Sprang et al., 1982). For D-gluconolactone, inhibition constants of 1 mM with phosphorylase *b* (Tu et al., 1971) and 7.5 mM and 0.69 mM with phosphorylase *a* and phosphorylase *a*–glycogen complexes, respectively (Gold et al., 1971), have been reported. Thus PUG binds considerably better than glucose and shows greater affinity than D-gluconolactone, most likely because of the additional interactions made by the *N*-phenylurethane component. The synergistic inhibition observed with caffeine supports the notion that PUG is a T-state inhibitor. However, analysis of the interaction constant suggested that the binding of one inhibitor did not influence the binding of the other ligand in contrast to the stronger synergism observed in the case of glucose and caffeine.

The phosphorylase reaction proceeds through a random equilibrium bi-bi kinetic mechanism in which the rate-limiting step is the interconversion of the ternary enzyme substrate complex [reviewed by Graves and Wang (1972)]. The reaction results in retention of configuration and is assumed to proceed through a glucosyl oxocarbonium ion intermediate [evidence reviewed by Johnson et al. (1988b)]. Transition-state theory suggests that an enzyme should show an increased affinity for the transition state compared to substrate that should be similar in magnitude to the catalytic rate enhancement of the enzyme (Pauling, 1946; Wolfenden, 1969). Hence, following successful studies with the β-glycosidases, the inhibitory properties of compounds such as D-gluconolactone whose structures resemble the half-chair conformation of the proposed oxocarbonium ion transition state have been investigated. The

kinetic studies have shown that D-gluconolactone (Tu et al., 1971; Gold et al., 1971), heptenitol (Klein et al., 1986), and PUG (present work) are effective inhibitors but do not exhibit the tight binding anticipated for transition-state analogues. This would suggest that for single substrate binding the catalytic site has no great preference for a half-chair or chair conformation of a glucosyl residue.

This observation is supported by the crystallographic studies. Comparison of the interactions made between phosphorylase *b* and sugars which bind in the chair conformation (e.g., glucose, glucose-1-P, heptulose-2-P) and those between phosphorylase *b* and glucosyl analogues which adopt a half-chair conformation (e.g., heptenitol and PUG) shows no large differences in either favorable or unfavorable interactions between the protein and the sugar component that would distinguish between half-chair or chair conformations. Moreover, there are no negatively charged groups in the vicinity of the O5 and C1 atoms that would favor an oxocarbonium ion intermediate. The groups that are closest to these atoms are Leu 136 and His 377. Although in the crystal structure phosphorylase is in the T state, the enzyme is catalytically active, and at high substrate concentrations the activity of the IMP-activated enzyme approaches that of the AMP-activated enzyme.

The absence of such constraints is consistent with stereoelectronic theory (Deslongchamps, 1983; Kirby, 1986; Gorenstein, 1987). The theory predicts that there is a stereoelectronic barrier to the cleavage of an equatorial glycoside that is absent for the axial isomer. In the ground-state conformation of a β-D-glycoside the C1–O bond is equatorial and antiperiplanar only to ring bonds so that C–OR cleavage is predicted to be unfavorable. The reaction can be made more favorable by distortion to a half-chair or sofa conformation. For α-D-glycosides, on the other hand, a lone pair of electrons of the ring oxygen possesses an antiperiplanar orientation to the C–OR bond so that C–OR cleavage is stereoelectronically favorable in the ground-state conformation. Hence there may not be the obligation for α-glycoside recognition enzymes to favor a distorted conformation of the glucopyranose ring in contrast to the situation for β-glycoside recognition enzymes where, for example, in the case of lysozyme there is experimental evidence that the sofa conformation of the glucosyl residue is preferred (Phillips, 1967; Imoto et al., 1972; Ford et al., 1974).

Consideration of the possible modes of binding of oligosaccharide substrates supports the notion that the enzyme does not favor distortion of the substrate. Phosphorylase has a strong glucosyl recognition site but a rather poor recognition site for oligosaccharide. It is fair to assume therefore that the non-reducing-end terminal glucose is the most firmly bound and that the location of this residue determines the direction of the rest of the oligosaccharide. If the terminal sugar has a half-chair conformation with trigonal geometry at C1, then the oligosaccharide is directed into the PUG channel (channel 1), which, as the present studies show, is available in the T-state enzyme but which has no access to the surface. On the other hand, if the terminal sugar has a chair conformation with tetrahedral geometry at C1, then the oligosaccharide is directed toward channel 2, which, on the basis of observations made with R-state inhibitors (Hajdu et al., 1987; Oikonomakos et al., 1988), becomes available on the T to R conversion and leads to access to the surface.

The preliminary kinetic studies reported here indicate that, in solution with the R-state enzyme, maltose is a poor inhibitor compared with glucose and that maltotriose is a better inhibitor than maltose but still is not as effective as glucose. The results suggest that the recognition site for the second sugar at the catalytic site is poor and may involve some steric conflict which may be partially compensated by binding the third sugar.

The combination of crystallographic and kinetic studies with stereochemical considerations suggests that the phosphorylase mechanism does not need nor does it involve the distortion of the terminal sugar of the oligosaccharide (or of glucose-1-P) before bond breaking. However, interactions that both favor and stabilize the oxocarbonium ion intermediate undoubtedly play an important role in catalysis. In the reaction mechanism proposed by the Würzburg and Oxford groups (Feldman et al., 1978; McLaughlin et al., 1984; Klein et al., 1986; Hajdu et al., 1987) the 5′-phosphate of the cofactor pyridoxal phosphate acts as a general acid which promotes the attack of inorganic phosphate on the glycosidic bond of the glycogen substrate. Following protonation of the glycosidic oxygen and subsequent cleavage of the C1–O bond the oxocarbonium ion intermediate is stabilized by the inorganic phosphate dianion itself. The reaction is completed by nucleophilic attack of the phosphate on the carbonium ion. Thus in this mechanism the attacking group of the substrate, promoted by its interactions with the cofactor and protein, serves to stabilize and favor the transition-state intermediate. Gold et al. (1971) have shown that D-gluconolactone binds most strongly to the enzyme–glycogen–P_i complex (K_{APi} = 0.025 mM), a result that supports these proposals. Moreover in the heptenitol reaction, it is heptulose-2-P and not heptenitol that is the transition-state analogue (Klein et al., 1986; McLaughlin et al., 1984; Hajdu et al., 1987), a result that also indicates a key role for the substrate phosphate.

ACKNOWLEDGMENTS

We are grateful to Dr. D. I. Stuart for his outstanding contribution to the refinement of the crystal structure of phosphorylase and to Dr. P. J. McLaughlin for his help with computing.

REFERENCES

Beer, D., & Vasella, A. (1985) *Helv. Chim. Acta 68*, 2254–2274.

Beer, D., & Vasella, A. (1986) *Helv. Chim. Acta 69*, 267–270.

Connolly, M. L. (1985) *J. Am. Chem. Soc. 107*, 1118–1124.

Deslongchamps, P. (1983) *Stereoelectronic Effects in Organic Chemistry*, Pergamon, Oxford.

Dombradi, V. (1981) *Int. J. Biochem. 13*, 125–139.

Engers, H. D., Shechosky, S., & Madsen, N. B. (1970) *Can. J. Biochem. 48*, 746–754.

Feldman, K.; Horl, M., Klein, H. W., & Helmreich, E. J. M. (1978) *Proc. Natl. Acad. Sci. U.S.A. 74*, 856–860.

Fischer, E. H., & Krebs, E. G. (1962) *Methods Enzymol. 5*, 369–373.

Fiske, C. H., & Subbarow, Y. (1925) *J. Biol. Chem. 66*, 375–400.

Ford, L. O., Johnson, L. N., Machin, P. A., Phillips, D. C., & Tjian, T. (1974) *J. Mol. Biol. 88*, 349–371.

Frauenfelder, H., Hartmann, H., Karplus, M., Kuntz, I. D., Kuriyan, J., Parak, F., Petsko, G. A., Ringe, D., Tilton, R. F., Connolly, M. L., & Max, N. (1987) *Biochemistry 26*, 254–261.

Gold, A. M., Legrand, E., & Sanchez, G., (1971) *J. Biol. Chem. 246*, 5700–5706.

Goldsmith, E. J., & Fletterick, R. J. (1983) *Pure Appl. Chem. 55*, 577–588.

Gorenstein, D. G. (1987) *Chem. Rev. 87*, 1047–1077.

Graves, D. J., & Wang, J. H. (1972) *Enzymes (3rd Ed.) 7*, 435–482.
Hackert, M. L., & Jacobson, R. A. (1971) *Acta Crystallogr., Sect. B: Struct. Crystallogr. Cryst. Chem. B27*, 203–209.
Hajdu, J., Acharya, K. R., Stuart, D. I., McLaughlin, P. J., Barford, D., Oikonomakos, N. G., Klein, H. W., & Johnson, L. N. (1987) *EMBO J. 6*, 539–546.
Helliwell, J. R., Papiz, M. Z., Glover, I. D., Habash, J., Thompson, A. W., Moore, P. R., Harris, N., Croft, D., & Pantos, E. (1986) *Nucl. Instrum. Methods Phys. Res., Sect. A 246*, 617–623.
Hol, W. G. J. (1986) *Angew. Chem., Int. Ed. Engl. 25*, 767–778.
Hu, H.-Y., & Gold, A. M. (1975) *Biochemistry 14*, 2224–2230.
Imoto, T., Johnson, L. N., North, A. C. T., Phillips, D. C., & Rupley, J. A. (1972) *Enzymes (3rd Ed.) 7*, 665–867.
Jenkins, J. A., Johnson, L. N., Stuart, D. I., Stura, E. A., Wilson, K. S., & Zanotti, G. (1981) *Philos. Trans. R. Soc. London, B 293*, 23–41.
Johnson, L. N., Madsen, N. B., Mosley, J., & Wilson, K. S. (1974) *J. Mol. Biol. 90*, 703–717.
Johnson, L. N., Jenkins, J. A., Wilson, K. S., Stura, E. A., & Zanotti, G. (1980) *J. Mol. Biol. 140*, 565–580.
Johnson, L. N., Stura, E. A., Sansom, M. S. P., & Babu, Y. S. (1983) *Biochem. Soc. Trans. 11*, 142–144.
Johnson, L. N., Cheetham, J. C., Mclaughlin, P. J., Acharya, K. R., Barford, D., & Phillips, D. C. (1988a) *Curr. Top. Microbiol. Immunol.* (in press).
Johnson, L. N., Hajdu, J., Acharya, K. R., Stuart, D. I., McLaughlin, P. J., Oikonomakos, N. G., & Barford, D. (1988b) in *Allosteric Enzymes* (Herve, G., Ed.) CRC Press, Boca Raton, FL (in press).
Jones, T. A. (1978) *J. Appl. Crystallogr. 11*, 272–288.
Jones, T. A. (1985) *Methods Enzymol. 115*, 157–171.
Kasvinsky, P. J., & Madsen, N. B. (1976) *J. Biol. Chem. 251*, 6852–6859.
Kasvinsky, P. J., Madsen, N. B., Sygusch, J., & Fletterick, R. J. (1978a) *J. Biol. Chem. 253*, 3343–3351.
Kasvinsky, P. J., Shechosky, S., & Fletterick, R. J. (1978b) *J. Biol. Chem. 253*, 9102–9106.
Kirby, A. J. (1987) *Crit. Rev. Biochem. 22*, 283–315.
Klein, H. W., Im, M. J., & Palm, D. (1986) *Eur. J. Biochem. 157*, 107–114.
Lee, B. K., & Richards, F. M. (1971) *J. Mol. Biol. 55*, 379–400.
Madsen, N. B. (1986) *Enzymes (3rd Ed.) 17*, 365–394.
Madsen, N. B., Kasvinsky, P. J., & Fletterick, R. J. (1978) *J. Biol. Chem. 253*, 9097–9101.
Madsen, N. B., Shechosky, S., & Fletterick, R. J. (1983) *Biochemistry 22*, 4460–4465.
McLaughlin, P. J., Stuart, D. I., Klein, H. W., Oikonomakos, N. G., & Johnson, L. N. (1984) *Biochemistry 23*, 5862–5873.
Nybourg, J., & Wonacott, A. J. (1977) in *The Rotation Method in Crystallography* (Arndt, U. W., & Wonacott, A. J., Eds.) pp 139–152, North-Holland, Amsterdam.
Oikonomakos, N. G., Johnson, L. N., Acharya, K. R., Stuart, D. I., Barford, D., Hajdu, J., Varvill, K. M., Melpidou, A. E., Papageorgiou, T., Graves, D. J., & Palm, D. (1987) *Biochemistry 26*, 8381–8389.
Oikonomakos, N. G., Acharya, K. R., Stuart, D. I., Melpidou, A. E., Mclaughlin, P. J., & Johnson, L. N. (1988) *Eur. J. Biochem. 173*, 569–578.
Pauling, L. (1946) *Chem. Eng. News 24*, 1375–1377.
Phillips, D. C. (1967) *Proc. Natl. Acad. Sci. U.S.A. 57*, 484–495.
Rashin, A. A., Iofin, M., & Honig, B. (1986) *Biochemistry 25*, 3619–3625.
Richards, F. M. (1974) *J. Mol. Biol. 82*, 1–14.
Sansom, M. S. P., Stuart, D. I., Acharya, K. R., Hajdu, J., McLaughlin, P. J., & Johnson, L. N. (1985) *J. Mol. Struct. 123*, 3–25.
Segal, I. H. (1975) *Enzyme Kinetics*, pp 481–487, Wiley-Interscience, New York.
Sprang, S. R., & Fletterick, R. J. (1979) *J. Mol. Biol. 131*, 523–551.
Sprang, S. R., Goldsmith, E. J., Fletterick, R. J., Withers, S. G., & Madsen, N. B. (1982) *Biochemistry 21*, 5364–5371.
Tilton, R. F., Kuntz, I. D., & Petsko, G. A. (1984) *Biochemistry 23*, 2849–2857.
Tilton, R. F., Singh, U. C., Kuntz, I. D., & Kollman, P. A. (1988) *J. Mol. Biol. 199*, 195–211.
Tu, J.-I., Jacobson, G. R., & Graves, D. J. (1971) *Biochemistry 10*, 1229–1236.
Withers, S. G., Madsen, N. B., Sprang, S. R., & Fletterick, R. J. (1982) *Biochemistry 21*, 5372–5382.
Wolfenden, R. (1969) *Nature (London) 223*, 704–705.